Extended Abstracts of the 2019 International Conference on Solid State Devices and Materials, Nagoya, 2019, pp887-888

SiC Quantum Dots in Si-Oxide Layer Fabricated by Double Hot-Si^+/C^+-Ion Implantation Technique

T. Mizuno, R. Kanazawa, T. Aoki, and T. Sameshima*
Kanagawa Univ., Hiratsuka, Japan (mizuno@kanagawa-u.ac.jp), * Tokyo Univ. of Agric. and Tech., Koganei, Japan

Abstract

We experimentally studied SiC quantum nano-dots in Si-oxide layer fabricated by double hot-Si^+/C^+ ion implantation technique (Si^+/C^+-OX), comparing with SiC dots by single hot-C^+ ion implanted oxide (C^+-OX) and amorphous-Si layers (C^+-aSi). STEM analysis shows that SiC dots were successfully formed in Si^+/C^+-OX. The Raman peaks of T- and D-bands of a-carbon (a-C), as well as TO-mode of Si-C vibration, are observed in Si^+/C^+-OX, which is the direct verification of SiC and a-C formation. We demonstrated that the maximum PL intensity I_{PL} of Si^+/C^+-OX is approximately 1.7 and 8.7 times larger than those of C^+-aSi and C^+-OX, respectively. The PL peak energy of Si^+/C^+-OX (2.5eV) is lower than that of C^+-aSi (3.1eV). The I_{PL} of Si^+/C^+-OX shows the rapid increase after N_2 annealing, which is possibly attributable to the PL quantum efficiency enhancement of SiC dot.

I. Introduction

Using the self-cluster effects of ion-implanted C atoms in Si [1], 3C-SiC and hexagonal-SiC (H-SiC) nano-dots (diameter R≈2nm) can be easily formed even in amorphous-Si layer (a-Si) as well as polysilicon (poly-Si) and crystal-Si (c-Si) by hot-C^+-ion implantation technique [2], [3]. Thus, the crystal structure of Si is not essential for the SiC dot formation by hot-C^+-ion implantation. We demonstrated the very large bandgap E_G (≈3eV) (≡peak PL-wavelength λ_{PL} of 400nm) and very strong PL emission I_{PL} in the near-UV/visible regions (>400nm) from indirect-bandgap SiC dots, which is possibly attributable to free exciton recombination of excited electrons in SiC dots [4]. However, since the SiC dots with large E_G are embedded in Si layer with small E_G (≈1.1eV), the SiC dot in Si layer is not a quantum dot, resulting in small PL quantum efficiency for visible Si-based photonic devices. Thus, it is strongly required to realize a quantum SiC dot embedded in much larger E_G material, such as SiO_2 with E_G≈9eV, and thus the PL quantum efficiency of quantum SiC dots can be improved by band-to-band recombination of excited electrons.

In this work, we experimentally studied the SiC quantum dots embedded in SiO_2, using double hot-Si^+/C^+-ion implantation into a surface-SiO_2 (Si^+/C^+-OX) on bulk-Si. We successfully improved the PL intensity I_{PL} of quantum SiC dots in Si^+/C^+-OX, compared to those of single hot-C^+-ion implanted oxide (C^+-OX) and a-Si layers (C^+-aSi). Moreover, an a-carbon (a-C) in C^+-OX also showed very broad PL spectrum, as reported [5], but the I_{PL} was very weak.

II. Experiment Procedure

To form a SiC dot in surface-SiO_2 (SOX) layer, Si atoms as well as C atoms are required to coexist in SOX. SiC quantum dots in SOX were fabricated by double hot-ion implantations of Si^+ **(Fig.1-(I)(b))** and C^+ ion **(Fig.1-(I)(c))** into the SOX layer on (100) bulk-Si substrate at substrate temperature T (600°C) after forming 140-nm thick SOX **(Fig.1-(I)(a))**, using low and high hot-ion dose conditions of Si^+ (D_S) and C^+-ion doses (D_C) for Si^+/C^+-OX **(Table-1)**. As a result, the peak concentrations of Si and C atoms at low dose conditions, simulated by Monte-Carlo simulator SRIM [6], are to be approximately 7×10^{21} and 5×10^{21} cm^{-3}, respectively **(Fig.2)**. Post N_2 annealing was carried out at annealing temperature T_N=1000°C for various annealing time t_N ($0<t_N\leq60$min), to poly-crystallize implanted Si atoms in SOX **(Fig.1-(I)(d)**, because a-Si can be poly-crystallized [3]. C^+-OX structure was also formed in SOX **(Fig.1-(II)(a))**, using the single hot-C^+ ion implantation **(Fig.1-(II)(b))** and post N_2 annealing **(Fig.1-(II)(c))**. SiC dots in C^+-aSi were also fabricated by hot-C^+-ion implantation into a-Si layer [3].

PL and Raman properties of three structures **(Table-1)** were measured at room temperatrure, where the excitation laser energy and diameter were 3.8eV and 1μm, respectively. The PL spectrum in the wide range of λ_{PL} from the UV to NIR regions was calibrated using a standard illuminant.

III. Results and Discussions

A. Material Structures of Si^+/C^+-OX and C^+-OX

Since SiC dots are local Si-rich areas in SOX, SiC dot areas in HAADF-STEM image for Si^+/C^+-OX shows bright areas. Actually, STEM image shows that many SiC dots with R≈2-4nm (bright areas encircled in **Fig. 3**) are successfully observed below the 30nm depth from the SOX surface, whose C content in the SiC-dot layer is estimated to higher than 2at.% **(Fig.2)**. However, in Si layer, SiC-dots were not formed, because of very low C-content (<1.5at.%) **(Fig.2)**.

It is noted that UV-Raman analysis of Si^+/C^+-OX **(Fig.4)** shows the strong two peaks of the T-band around 1100cm^{-1} [7] and D-band of C-C vibration and no G-band peak, which suggests that a-C in Si^+/C^+-OX mainly consists of diamond-like carbon (sp^3 site) [5]. However, the TO-mode (I_{TO}) of Si-C vibration is very weak, compared with those of C^+-aSi.

Moreover, with increasing the ion dose, the Raman intensities I_R of both T- and D-bands increase, and especially the D-band intensity enhancement is much larger than the T-band enhancement **(Figs. 5(a) and 5(b))**. Moreover, all I_R-peaks decrease with increasing t_N under low ion dose conditions in $t_N\leq$30min **(Fig. 5(b))**, whereas I_D, I_T, and I_{TO} peaks at high dose conditions are almost independent of t_N. Thus, at low ion dose conditions, it is possible that a-C area reduces after N_2 annealing.

On the other hand, C^+-OX shows the typical Raman spectrum of a-C including the G-band of graphite (sp^2 site) **(Fig.6).** The I_D of Si^+/C^+-OX is much smaller than of that of C^+-OX, which indirectly suggests that some C atoms of Si^+/C^+-OX bind to Si atoms, resulting in SiC dot formation. However, the TO mode of Si-C vibration cannot been observed in C^+-OX, as expected.

B. PL Properties of Si^+/C^+-OX and C^+-OX

Firstly, we discuss the PL properties under low ion dose conditions. We successfully demonstrated that the PL intensity I_{PL} of Si^+/C^+-OX is much larger than that of C^+-aSi, and the peak PL energy E_{PH} exhibits a red-shift from approximately 3.1eV of C^+-aSi to 2.5eV **(Fig.7)**. The broad PL of C^+-OX is also observed, but the PL intensity is one order of magnitude smaller than that of Si^+/C^+-OX even under the same D_C **(Fig.7)** .

The I_{PL} of Si^+/C^+-OX is remarkably enhanced after N_2 annealing **(Fig.8)**, and drastically increase with increasing t_N under $t_N\leq$30min. As a result, the maximum I_{PL} of Si^+/C^+-OX is approximately 1.7 and 8.7 times larger than those of C^+-aSi and C^+-OX, respectively. The I_{PL} enhancement factor ΔI_{PL} compared with I_{PL} at t_N=0 amounts to approximately 9.5 at t_N=30min, which is much larger than the ΔI_{PL} of C^+-aSi (2.8) and C^+-OX (2.2). The I_{PL} of Si^+/C^+-OX negatively correlates to the I_R of C-C and Si-C vibrations **(Fig.5(b))**, which suggests that the PL quantum efficiency of SiC dots increases after N_2 annealing. In addition, the I_{PL} of C^+-OX is still lower than the I_{PL} of Si^+/C^+-OX in spite of increasing t_N, which indicates that the I_{PL} of a-C in C^+-OX is much smaller than that of SiC dots.

Secondly, we discuss the hot-ion dose dependence of PL properties of Si^+/C^+-OX.

In spite of increasing D_C, the I_{PL} of Si^+/C^+-OX is reduced, which is approximately 85% of that at low D_C **(Fig.9(a))**. However, the PL spectrum line shape is independent of D_C **(Fig.9(a))**. In addition, the t_N dependence of the I_{PL} improvement of Si^+/C^+-OX at high D_C is very slow, and the maximum I_{PL} improvement can be achieved at t_N=240min, whereas the peak-t_N under low D_C is only 30min **(Fig.9(b))**. Thus, it is strongly required to optimize the hot-ion dose to improve the I_{PL} of Si^+/C^+-OX.

IV. Conclusion

In this work, we experimentally studied SiC quantum dots in SOX fabricated by the double hot-Si^+/C^+ implantation into an oxide layer. We demonstrated very strong PL intensity of Si^+/C^+-OX in the UV/visible regions, compared with that of C^+-aSi and C^+-OX. Since a semiconductor layer is not essential for forming Si^+/C^+-OX, Si^+/C^+-OX technique is very promising for low-cost visible photonic devices.

Acknowledgement: This work was partially supported by KAKENHI (17K06359).

References: [1] T.Mizuno, JJAP **57**, 04FB03, 2018. [2] T.Mizuno, Abst. SNW, p.121, 2018. [3] T.Mizuno, JJAP **58**, SBBJ01, 2019. [4] J.Fan, *Silicon Carbide Nanostructures* (Springer), 2014. [5] Rusli, JAP **80**, 2998, 1996. [6] J.F.Ziegler, http://www.srim.org/. [7] C. Casiraghi, Phys. Rev. **B 72**, 085401, 2005.

Structures	D_S ($\times10^{16}$cm^{-2})	D_C ($\times10^{16}$cm^{-2})
Si$^+$/C$^+$-OX	6	4
	10	6
C$^+$-OX	0	4
C$^+$-aSi	0	4

Table-1 Hot-ion dose conditions for three structures.

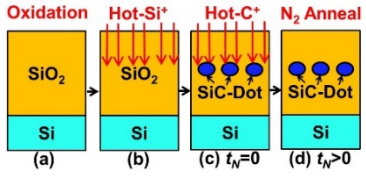

(I) Si$^+$/C$^+$-OX

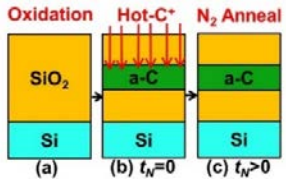

(II) C$^+$-OX

Fig.1 Fabrication steps for (I) Si$^+$/C$^+$-OX by double hot-Si$^+$/C$^+$-ion-implantation into SOX and (II) C$^+$-OX by single hot-C$^+$-ion-implantation into SOX. In (I), after (a) forming 140-nm thick SiO_2 on (100) bulk-Si substrate, (b) hot-Si$^+$-ions and (c) the following hot-C$^+$-ions were implanted into the SOX layer at T=600°C. (d) Post N_2 annealing was carried out at T_N=1000°C for annealing time t_N. (II) shows that C$^+$-OX is also fabricated by the same processes for Si$^+$/C$^+$-OX without hot-Si$^+$-ion implantation of (I)-(b).

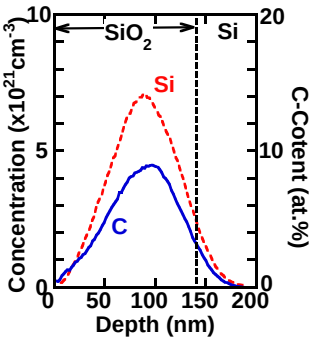

Fig.2 Implanted Si (dashed line) and C atom (solid line) depth profiles simulated by SRIM [6], where D_S=6×10^{16} cm^{-2}, D_C=4×10^{16} cm^{-2}, and T=25°C. The left and right vertical axes show the concentration and C-content, respectively.

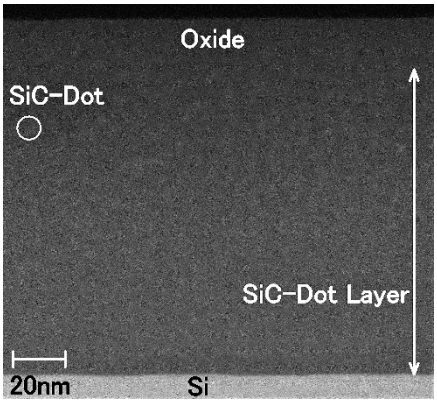

Fig.3 HAADF-STEM images of the cross section of SiC dots (bright areas) encircled in SOX of Si$^+$/C$^+$-OX, where D_S=6×10^{16}cm^{-2}, D_C=4×10^{16} cm^{-2}, and t_N=10min. SiC dots in SOX are the Si rich area, resulting in the bright areas in HAADF-STEM image. Many SiC dots are formed below 30nm depth from the SOX surface shown as an arrow of SiC-Dot Layer.

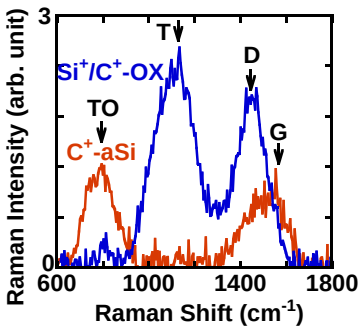

Fig.4 Raman spectra of Si$^+$/C$^+$-OX (blue line) at D_S=6×10^{16}cm^{-2} and C$^+$-aSi (brown line), where D_C=4×10^{16} cm^{-2} and t_N=0. The arrows of Si$^+$/C$^+$-OX show the D and T bands of C-C vibration, and the arrows of C$^+$-aSi show the G band of C-C vibration and the TO mode of Si-C vibration.

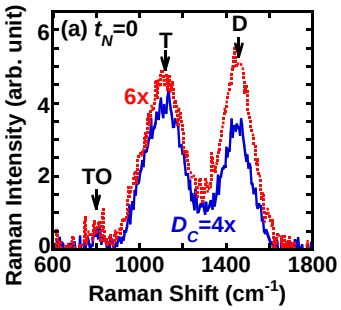

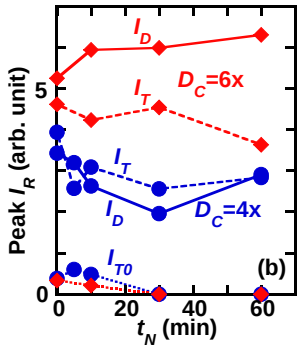

Fig.5 (a) D_C dependence of Raman spectra of Si$^+$/C$^+$-OX under low (D_S=6×10^{16}cm^{-2} and D_C=4×10^{16} cm^{-2} (solid line)) and high ion dose conditions (D_S=1×10^{17}cm^{-2} and D_C=6×10^{16}cm^{-2} (dotted line)), where t_N=0. (b) t_N dependence of I_D (solid lines), I_T (dashed lines), and I_{TO} peaks (dotted lines) under low (circles) and high ion dose conditions (rhombi). At low ion dose, both I_D and I_T decrease after N_2 annealing at t_N≤30min. I_{TO} also decreases and is almost zero at t_N≥30min.

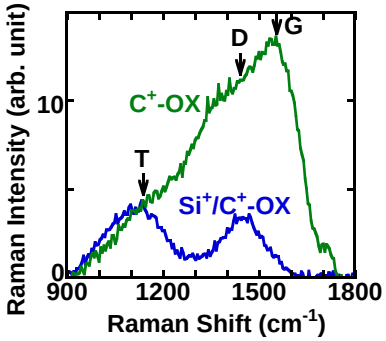

Fig.6 Raman spectra of Si$^+$/C$^+$-OX (blue line) at D_S=6×10^{16}cm^{-2} and C$^+$-OX (green line), where D_C=4×10^{16} cm^{-2} and t_N=0. The arrows show the G (observed in only C$^+$-OX), D and T bands of C-C vibration.

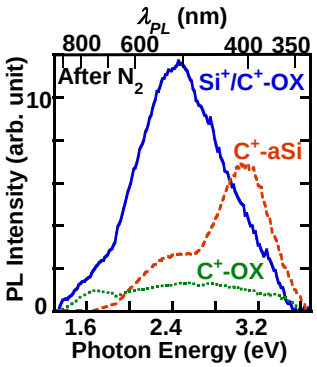

Fig.7 PL spectra of three structures of Si$^+$/C$^+$-OX at D_S=6×10^{16} cm^{-2} (solid line), C$^+$-aSi (dashed line), and C$^+$-OX (dotted line) after N_2 annealing, where D_C=4×10^{16} cm^{-2}. t_N of Si$^+$/C$^+$-OX, C$^+$-aSi, and C$^+$-OX are 30, 10, and 30min under the maximum I_{PL} conditions, respectively.

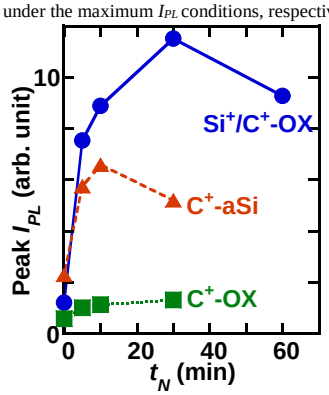

Fig.8 t_N dependence of peak-I_{PL} of Si$^+$/C$^+$-OX at D_S=6×10^{16} cm^{-2} (circles), C$^+$-aSi (triangles), and C$^+$-OX (squares), where D_C=4×10^{16} cm^{-2}.

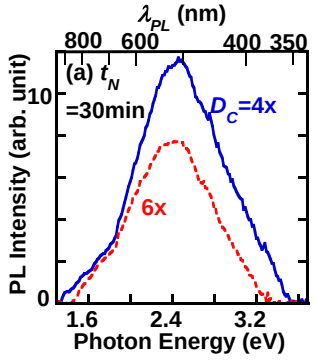

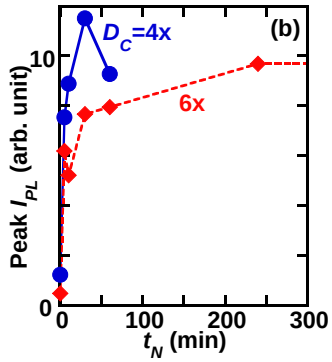

Fig.9 (a) D_C dependence of PL spectra under low (D_S=6×10^{16}cm^{-2} and D_C=4×10^{16} cm^{-2} (solid line)) and high ion dose conditions (D_S=1×10^{17}cm^{-2} and D_C=6×10^{16}cm^{-2} (dotted line)), where t_N=30min. (b) t_N dependence of peak-I_{PL} of Si$^+$/C$^+$-OX at low (circles) and high ion doses (rhombi).